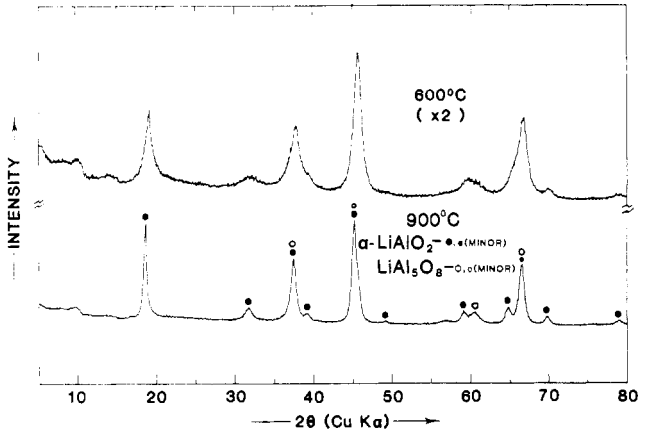

Figure 9. Powder X-ray diffraction pattern of $[LiAl_2(OH)_6]^+NO_3^-\cdot 0.5H_2O$ after calcination at 600 and 900 °C. The diffraction peaks of α-$LiAlO_2$ (●) and $LiAl_5O_8$ (○) are shown for the 900 °C sample.

stages as a function of temperature. Figure 2b illustrates the decomposition behavior of the nitrate compound as followed by thermogravimetric analysis.

Figure 7 illustrates powder X-ray diffraction patterns, recorded at ambient conditions, of the nitrate compound as prepared, and after calcination at 200, 400, 600, and 1100 °C. From the first stage of decomposition the thermal behavior of the nitrate is unlike that of the hydroxide, in that the nitrate can be dehydrated without significant structural changes. Upon further heating there is clear evidence for lithium nitrate and a poorly crystalline compound, perhaps an alumina. From Figure 8 we observe in more detail that at 300 °C the precursor is a mixture of dehydrated starting material, lithium nitrate, and a poorly crystalline spinel-like phase. After 400 °C was reached, the starting material has disappeared. By 600 °C the nitrate has decomposed and the mixture has reacted to form a mixture of α-$LiAlO_2$ and $LiAl_5O_8$ (3/1 molar ratio), which is stable up to 900 °C (see Figure 9). By 1100 °C α-$LiAlO_2$ has converted to γ-$LiAlO_2$ to form a mixture of γ-$LiAlO_2$ and $LiAl_5O_8$, the known compounds stable at high temperature in this region of the Li_2O-Al_2O_3 system.[21] Evidently, if a compound such as $Li_2Al_4O_7$ can be formed from the decomposition of $[LiAl_2(OH)_6]^+OH^-\cdot 2H_2O$, it will be unstable with respect to a mixture of α-$LiAlO_2$ and $LiAl_5O_8$ at intermediate temperatures and to the γ-form of $LiAlO_2$ at elevated temperature.

Acknowledgment. We thank the National Science Foundation and Northwestern Materials Research Center (Grant DMR 8520280) and Alcoa Foundation for their support of this research. K.R.P. thanks Du Pont for a Young Faculty Award.

Registry No. $Al(OH)_3$, 21645-51-2; $AlCl_3$, 7446-70-0; NH_4OH, 1336-21-6; LiOH, 1310-65-2; $[LiAl_2(OH)_6]^+OH^-\cdot 2H_2O$, 12344-53-5; $[LiAl_2(OH)_6]^+Cl^-\cdot nH_2O$ (n = 0.5), 110027-58-2; $LiOH\cdot H_2O$, 1310-66-3; LiCl, 7447-41-8; $LiAlO_2$, 12003-67-7; $LiAl_5O_8$, 12005-14-0; $Li_2Al_4O_7$, 12446-24-1; $[LiAl_2(OH)_6]^+NO_3^-\cdot 0.5H_2O$, 110027-60-6; $LiNO_3$, 7790-69-4.

Contribution from the Lehrstuhl für Anorganische Chemie I, Ruhr-Universität, D-4630 Bochum, FRG, and Anorganisch Chemisches Institut der Universität, D-6900 Heidelberg, FRG

General Route to μ-Hydroxo-Bis(μ-acetato)-Bridged Heterometal Dinuclear Complexes. Syntheses, Magnetic and Redox Properties, Electronic Spectra, and Molecular Structures of the Cr(III)-Co(II) and Cr(III)-Fe(II) Species

Phalguni Chaudhuri,*† Manuela Winter,† Heinz-Josef Küppers,† Karl Wieghardt,† Bernhard Nuber,‡ and Johannes Weiss‡

Received March 19, 1987

A series of heterodinuclear complexes of general formula $[LCr(\mu\text{-}OH)(\mu\text{-}CH_3COO)_2ML](ClO_4)_2$ (L = $C_9H_{21}N_3$, 1,4,7-trimethyl-1,4,7-triazacyclononane; M = Zn(II), Cu(II), Ni(II), Co(II), Fe(II), and Mn(II)) have been synthesized. The homodinuclear complex $[LCr(\mu\text{-}OH)(\mu\text{-}CH_3COO)_2CrL](ClO_4)_3$ has also been isolated. The crystal molecular structures of the Cr(III)-Fe(II) and Cr(III)-Co(II) complexes have been established by X-ray diffraction methods. Both of them crystallize in the triclinic system, space group C_i^1-$P\bar{1}$, with lattice constants a = 12.637 (4) Å, b = 16.254 (5) Å, c = 19.141 (7) Å, α = 84.68 (3)°, β = 73.92 (3)°, γ = 68.33 (2)°, and Z = 4 for the Cr(III)-Fe(II) species and a = 12.535 (4) Å, b = 16.263 (6) Å, c = 19.111 (8) Å, α = 84.66 (3)°, β = 74.27 (3)°, γ = 68.59 (3)°, and Z = 4 for the Cr(III)-Co(II) complex. Least-squares refinement of the structures led to a final R value of 0.087 for 5285 unique reflections and 0.083 for 8999 unique reflections in the case of the Cr(III)-Fe(II) and Cr(III)-Co(II) complexes, respectively. The structures consist of heteroatom binuclear cations $[LCr(\mu\text{-}OH)(\mu\text{-}CH_3COO)_2ML]^{2+}$ (M = Fe(II) or Co(II)), uncoordinated perchlorate anions, and water of crystallization. The metal centers Cr(III) and Fe(II) or Co(II) are linked together via a hydroxo bridge and two further acetate bridges; the geometry around each metal center is distorted octahedral. The perchlorate salts of other heterodinuclear complexes are isostructural with the Cr(III)-Fe(II) and Cr(III)-Co(II) complexes. They also crystallize in the triclinic system, space group C_i^1-$P\bar{1}$, with very similar unit cell dimensions. Variable-temperature (4-300 K) magnetic susceptibility measurements indicate that the spins of Cr(III) and M(II) or Cr(III) are weakly antiferromagnetically coupled. The electronic spectra have been measured both in the solid state and in solution, and they are very similar, indicating the presence of the stable moiety $[Cr^{III}(\mu\text{-}OH)(CH_3COO)_2M]^{2+}$, also in solution. The spin-flip $^4A_{2g} \rightarrow {}^2E_g$ transitions with intensity gain from exchange coupling have been observed for the homodinuclear Cr(III)-Cr(III) complex. Redox potentials for the couples Cr(III)-M(III)/Cr(III)-M(II) (M = Mn, Fe, or Co) vs. Fc^+/Fc^0 (Fc^0 = ferrocene) have been determined from their quasi-reversible cyclic voltammograms (+0.36, -0.05, and +0.03 V, respectively) in acetonitrile.

Introduction

Both homo- and heterodinuclear transition-metal complexes occupy an important position in modern inorganic chemistry. The impetus for the study of these complexes derives from the interests in connection with magnetic exchange interactions[1-4] and electron transfer between metal ions[5] and from their significance as models[6,7] for biological systems. New magnetic exchange path-

†Ruhr-Universität.
‡Anorganisch Chemisches Institut der Universität Heidelberg.

(1) *Magneto-Structural Correlations in Exchange Coupled Systems*; Willett, R., Gatteschi, D., Kahn, O., Eds.; NATO ASI Series C: Mathematical and Physical Science; Reidel: Dordrecht, The Netherlands, 1985; Vol. 140.
(2) Kahn, O. *Angew. Chem.* **1985**, *97*, 837-853.
(3) Timken, M. D.; Marritt, W. A.; Hendrickson, D. N.; Gagne, R. A.; Sinn, E. *Inorg. Chem.* **1985**, *24*, 4202-4208.

0020-1669/87/1326-3302$01.50/0

ways can be expected for heterodinuclear complexes, where unusual sets of magnetic orbitals can be brought in close proximity; hence, investigations of a series of heterodinuclear complexes might be more informative in comparison to those of the homodinuclear complexes. The field of the heterodinuclear complexes[8,9] with different paramagnetic centers is still limited today by the small number of known and fully structurally characterized compounds and by the relative difficulty of synthesizing new compounds.[10] One method for the synthesis of heterodinuclear complexes is to use tetradentate Schiff-base metal complexes[11] as ligands for a simple metal salt; it has been possible to bring pairs of similar or different metal atoms into close (ligand-bridged) proximity. Another method for obtaining mixed-metal complexes is to use a stepwise reaction of two different metal ions with a macrocyclic binucleating ligand[12] with either two equivalent or two inequivalent coordination sites.

In contrast, we have developed a strategy of general interest, based on a kinetically controlled synthetic route, to synthesize heterometal dinuclear complexes. This has been accomplished by using the cation $[LCr(solvent)_3]^{3+}$ as one of the reactants. L

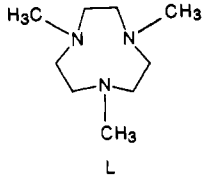

L

represents the simple tridentate cyclic amine 1,4,7-trimethyl 1,4,7-triazacyclononane, which coordinates facially in octahedral complexes. This ligand prevents for steric reasons the formation of ML_2 moieties, and only one ligand per metal center can be bound. We have already utilized the mentioned steric demand of this amine to synthesize the first structurally characterized triply hydroxo-bridged bimetallic complex of chromium(III)[13] and the only binuclear iron(II) complex[7] with a hydroxo bridge.

The subject of this paper is the syntheses of several dinuclear complexes containing 1,4,7-trimethyl-1,4,7-triazacyclononane as the terminal ligand and a hydroxo group and two acetate groups as bridging ligands: (1) the homodinuclear complex $[LCr^{III}(OH)(CH_3COO)_2Cr^{III}L](ClO_4)_3$; (2) the heterodinuclear complexes $[LCr^{III}(OH)(CH_3COO)_2M^{II}L](ClO_4)_2$ (where M = Zn, Cu, Ni, Co, Fe, and Mn). We also report their magnetic, spectroscopic, and electrochemical properties. Throughout this paper, the dinuclear complexes are denoted by the respective metal centers only; the terminal and bridging ligands are omitted for simplicity.

Experimental Section

The ligand 1,4,7-trimethyl-1,4,7-triazacyclononane (L) has been prepared by a procedure described elsewhere.[13] All other starting materials were commercially available. Microchemical carbon, hydrogen, and nitrogen analyses were performed by Beller Microanalytical Laboratory, Göttingen, West Germany. Electronic spectra were recorded on a Perkin-Elmer Lambda 9 spectrophotometer. Infrared spectra were recorded on a Beckmann Acculab 10 instrument (KBr disks). The magnetic susceptibilities of powdered samples were measured by using the Faraday method between 4 and 300 K. Diamagnetic corrections were applied using Pascal's constants. Cyclic voltammetric experiments were made with a Princeton Applied Research Model 173 potentiosat–galvanostat driven by a Model 175 universal programmer. Voltammograms were recorded on a Kipp & Zonen X-Y recorder, Model BD 90. A three-electrode cell with a Pt or an Au electrode as the working electrode, a platinum wire as the auxiliary electrode, and a Ag/AgCl electrode as the reference electrode was used for measurements. Tetrabutylammonium hexafluorophosphate was used as the supporting electrolyte.

$LCr(CO)_3$. A suspension of $Cr(CO)_6$ (2.20 g, 10 mmol) and the cyclic amine (L) (1.9 g, 11 mmol) was heated in 50 mL of mesitylene under gentle reflux for 40 min under argon. After the suspension was allowed to cool to room temperature, yellow orange microcrystals were filtered off, washed several times with small portions of benzene and ether, successively, and air-dried. The yield was between 75 and 85%. During the reaction, sublimation of $Cr(CO)_6$ occurred, varying the percentage of yield.

Anal. Calcd (found): C, 46.91 (46.0); H, 6.89 (6.81); N, 13.68 (13.70); Cr, 16.92 (16.1).

$LCrBr_3$. A suspension of $LCr(CO)_3$ (3.1 g, 10 mmol) in 50 mL of chloroform was treated with 1.5 mL of bromine dissolved in 20 mL of chloroform in a dropwise manner with continuous stirring. The mixture was refluxed for 30 min and then allowed to cool to room temperature. The green solid was filtered off, washed several times with chloroform, and air-dried. Yield: 3.80 g (82%).

Anal. Calcd (found): C, 23.35 (23.60); H, 4.57 (4.51); N, 9.08 (9.10); Cr, 11.23 (10.9).

Solution A. To a suspension of 0.46 g (1 mmol) of $LCrBr_3$ in 30 mL of absolute methanol was slowly added 0.62 g of $AgClO_4 \cdot H_2O$ (2.8 mmol) with stirring. The suspension was refluxed under argon for 30 min; during this time a blue-violet solution with a concomitant formation of AgBr resulted. Precipitated AgBr was filtered off, and the clear blue-violet solution was preserved in a dry condition for further use.

$[L_2Cr_2(\mu\text{-}OH)(\mu\text{-}CH_3COO)_2](ClO_4)_3$. Method 1. A sample of 0.20 g of anhydrous sodium acetate was added to the blue-violet solution A (see before), and the mixed solution was refluxed under argon for 1 h and then allowed to cool to room temperature. After addition of 0.4 g of $NaClO_4 \cdot H_2O$ to the solution, its volume was reduced by passing a stream of argon until red crystals precipitated out. The crystals were filtered off and air-dried. Yield: 0.35 g (80%).

Method 2. To a degassed solution of 50 mL of methanol containing 0.51 g (3 mmol) of cyclic amine, a sample of 0.27 g (1.5 mmol) $Cr(CH_3COO)_2 \cdot H_2O$ was added under stirring. The stirring was continued for 1 h, after which time 0.4 g of $NaClO_4 \cdot H_2O$ was added. The solution was filtered in the presence of air to get rid of any solid particles. Very slow evaporation of methanol by an argon stream yielded the crystals, which were collected by filtration and air-dried. Yield: 0.50 g (75%).

Anal. Calcd (found): C, 30.03 (29.6); H, 5.62 (5.54); N, 9.55 (9.50); Cr, 11.82 (10.9); ClO_4, 33.9 (30.8).

$[LCr^{III}(\mu\text{-}OH)(\mu\text{-}CH_3COO)_2Fe^{II}L](ClO_4)_2 \cdot 0.5H_2O$. All operations were done strictly under an argon atmosphere. To a rapidly stirred and degassed solution of 1,4,7-trimethyl-1,4,7-triazacyclononane (0.51 g, 3 mmol) in 50 mL of absolute methanol was added a sample of 0.36 g of $Fe(ClO_4)_2 \cdot 6H_2O$ (1 mmol). Stirring was continued further for 2.5 h until a clear deep blue solution was obtained. A sample of 0.2 g (2.44 mmol) of anhydrous sodium acetate was added to the blue solution, whereupon the color changed to pale yellow. The yellow solution was added to the degassed solution A (loc. cit.), and the mixed solution was refluxed for 20 min. After addition of 0.4 g of $NaClO_4 \cdot H_2O$ to the cooled solution, X-ray quality crystals were obtained by very slow evaporation of methanol by an argon stream. Yield: 0.38 g (48%).

Anal. Calcd (found): C, 33.68 (33.34); H, 6.30 (6.36); N, 10.71 (11.31); ClO_4, 25.36 (26.1); Cr, 6.63 (6.5); Fe, 7.12 (7.2).

$[LCr^{III}(\mu\text{-}OH)(\mu\text{-}CH_3COO)_2M^{II}L](ClO_4)_2$ (M = Zn, Cu, Ni, Co, Mn). Because all these complexes were prepared in a very similar way, a representative method only is described. An argon-scrubbed solution of the cyclic amine (0.34 g, 2 mmol) in 30 mL of methanol was treated with a sample of $M(CH_3COO)_2 \cdot xH_2O$ (1 mmol) under vigorous stirring in an argon atmosphere. After 0.5 h of stirring, the degassed solution A was added, followed by an addition of a solid sample of 0.4 g of $NaClO_4 \cdot H_2O$. The resulting solution was refluxed for 20 min. The volume of the solution was reduced by passing argon over the surface of the solution, until the crystals separated out. The crystals were collected by filtration and air-dried. Yield: 80–85%.

(4) Chaudhuri, P.; Oder, K.; Wieghardt, K.; Nuber, B.; Weiss, J. *Inorg. Chem.* **1986**, *25*, 2818–2824.
(5) Gagne, R. R.; Spiro, C. L.; Smith, T. J.; Hamann, C. A.; Thies, W. R.; Shiemke, A. K. *J. Am. Chem. Soc.* **1981**, *103*, 4073–4081.
(6) (a) Armstrong, W. H.; Lippard, S. J. *J. Am. Chem. Soc.* **1983**, *105*, 4837–4838. (b) Wieghardt, K.; Pohl, K.; Gebert, W. *Angew. Chem., Int. Ed. Engl.* **1983**, *22*, 727. (c) Wieghardt, K.; Bossek, U.; Ventur, D.; Weiss, J. *J. Chem. Soc., Chem. Commun.* **1985**, 347–349.
(7) Chaudhuri, P.; Wieghardt, K.; Nuber, B.; Weiss, J. *Angew. Chem., Int. Ed. Engl.* **1985**, *24*, 778–779.
(8) Bencini, A.; Caneschi, A.; Dei, A.; Gatteschi, D.; Zanchini, C.; Kahn, O. *Inorg. Chem.* **1986**, *25*, 1374–1378 and references therein.
(9) Mikuriya, M.; Okawa, H.; Kida, S.; Ueda, I. *Bull. Chem. Soc. Jpn.* **1978**, *51*, 2920–2923 and references therein.
(10) Casellato, U.; Vigato, P. A.; Fenton, D. E.; Vidali, M. *Chem. Soc. Rev.* **1979**, *8*, 199–220.
(11) (a) Gruber, S. J.; Harris, C. M.; Sinn, E. *J. Inorg. Nucl. Chem.* **1968**, *30*, 1805–1830. (b) Selbin, J.; Ganguly, L. *Inorg. Nucl. Chem. Lett.* **1969**, *5*, 815–818.
(12) (a) Pilkington, N. H.; Robson, R. *Aust. J. Chem.* **1979**, *23*, 2225–2236. (b) Okawa, H.; Tanaka, M.; Kida, S. *Chem. Lett.* **1974**, 987–988. (c) Lintvedt, R. L.; Glick, M. D.; Tomlonovic, B. K.; Gavel, D. P. *Inorg. Chem.* **1976**, *15*, 1646–1653.
(13) Wieghardt, K.; Chaudhuri, P.; Nuber, B.; Weiss, J. *Inorg. Chem.* **1982**, *21*, 3086–3090.

Table I. Summary of Crystal Data and Intensity Measurements

	Cr(III)–Co(II)	Cr(III)–Fe(II)
mol formula	$[CrCoC_{22}H_{49}N_6O_{13}Cl_2]\cdot 0.5H_2O$	$[CrFeC_{22}H_{49}N_6O_{13}Cl_2]\cdot 0.5H_2O$
cryst system	triclinic	triclinic
a, Å	12.535 (4)	12.637 (4)
b, Å	16.263 (6)	16.254 (5)
c, Å	19.111 (8)	19.141 (7)
α, deg	84.66 (3)	84.68 (3)
β, deg	74.27 (3)	73.92 (3)
γ, deg	68.59 (3)	68.33 (2)
V, Å	3491 (2)	3511 (2)
Z	4 (2 × 2)	4 (2 × 2)
space group	$P\bar{1}$ (C_i^1)	$P\bar{1}$ (C_i^1)
d, g cm^{-3}	1.515	1.50
diffractometer	Syntex R3 graphite monochromator	Syntex R3 graphite monochromator
μ(Mo Kα), cm^{-1}	9.97	9.34
data collcn mode	θ–2θ	θ–2θ
2θ range, deg	2.5–60	3–57
octants collcd	$\pm h,\pm k,l$	$\pm h,\pm k,l$
no. of reflcns measd	9718	5538
no. of reflcns used	8999 [$I \geq 2.5\sigma(I)$]	5285 [$I \geq 2\sigma(I)$]
no. of refined params	735	561
transmission factors: min; max	0.77; 1.00	0.85; 1.00
shift/esd: mean; max	0.07; 0.59	0.25; 1.05
residual peaks, e/Å^3: max; min	1.5; –0.91	1.6; –0.85
R^a	0.084	0.095
R_w^b	0.083	0.087
weighting factor w_i	$1/\sigma(F)^2$	$1/\sigma^2(F)$

$^a R = \sum||F_o| - |F_c||/\sum|F_o|$. $^b R_w = [\sum w_i(||F_o| - |F_c||)^2/\sum w_i|F_o|^2]^{1/2}$.

All of the isolated solid complexes are fairly air-stable and red-violet in color, except the Cr(III)–Zn(II) complex, which is light red.

Anal. Calcd (found) for Cr(III)–Mn(II): C, 33.73 (33.91); H, 6.30 (6.51) N, 10.73 (10.55); ClO_4, 25.39 (25.1); Cr, 6.64 (6.5). Calcd (found for Cr(III)–Co(II): C, 33.56 (33.4); H, 6.27 (6.20); N, 10.67 (10.6); ClO_4, 25.26 (24.7); Cr, 6.6 (6.7). Calcd (found) for Cr(III)–Ni(II): C, 33.56 (34.28); H, 6.27 (6.64); N, 10.68 (10.82); ClO_4, 25.3 (25.4); Cr, 6.61 (6.8). Calcd (found) for Cr(III)–Cu(II): C, 33.36 (32.86); H, 6.24 (6.21); N, 10.61 (10.51); ClO_4, 25.1 (24.6); Cr, 6.56 (6.9). Calcd (found) for Cr(III)–Zn(II): C, 33.28 (33.04); H, 6.22 (6.09); N, 10.59 (10.52); ClO_4; 25.05 (25.0); Cr, 6.55 (6.7).

Caution! Although we have experienced no difficulties with the perchlorate salts described here, these should be regarded as potentially explosive and handled accordingly.

X-ray Structure Determinations. A crystal (0.2 × 0.2 × 0.25 mm^3) of $[LCr(OH)(CH_3COO)_2FeL]_2(ClO_4)_4\cdot H_2O$ and a crystal (0.3 × 0.5 × 0.35 mm^3) of $[LCr(OH)(CH_3COO)_2CoL]_2(ClO_4)_4\cdot H_2O$ were attached to the end of a glass fiber and mounted on a Syntex R3 four-circle diffractometer. The unit cell parameters were obtained at 23 °C by a least-squares refinement of the angular settings of 25 reflections in each case. The data are summarized in Table I along with details of the treatment of intensity data. An empirical absorption correction was carried out.[14] The scattering factors[15] for neutral non-hydrogen atoms were corrected for both the real and the imaginary components of anomalous dispersion. The function minimized during least-squares refinements was $\sum w_i(|F_o| - |F_c|)^2$. The structures were solved via three-dimensional Patterson and Fourier syntheses. For The Cr(III)–Fe(II) complex, idealized positions of H atoms bound to carbon atoms were calculated (on the basis of d(C-H) = 0.97 Å and regular tetrahedral geometry about the C atoms) and included in the refinement[14] cycles with a common isotropic thermal parameter (U = 0.085 (5) Å^2). Refinements for the Cr(III)–Co(II) complex were carried out with anisotropic thermal parameters for all non-hydrogen atoms. But isotropic thermal parameters for carbon atoms were used for refinement of the Cr(III)–Fe(II) structure. Final positional parameters for all non-hydrogen atoms are given in Tables II and III. Selected bond distances and bond angles are listed in Tables IV and V. Listings of thermal parameters, observed and calculated structure factors, and C–C and C–N bond distances are available as supplementary materials.

Scheme I

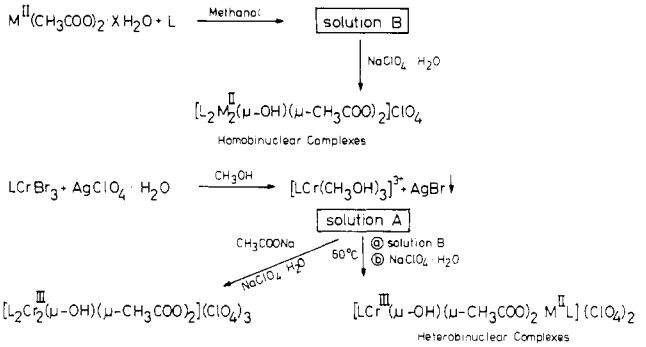

Results and Discussion

Synthesis. A straightforward, high-yield synthetic route to pure heterodinuclear complexes containing a μ-hydroxo bridge and two μ-acetate bridges has been developed, as outlined in Scheme I. The reactions are clean, affording large quantities of pure crystalline product in better than 80% yield. The kinetic inertness of trivalent chromium ion resulting from a d^3 electron configuration and the lability of the first transition series divalent metal ions are utilized to synthesize Cr(III)–M(II) binuclear complexes. Practically no scrambling was observed (vide infra)

$$2\text{Cr(III)–M(II)} \not\rightarrow \text{Cr(III)–Cr(III)} + \text{M(II)–M(II)}$$

probably because the reaction temperature was too low to surmount the activation barrier to dissociation. In contrast to other synthetic routes hitherto known[8,12] for mixed-metal complexes, it was not necessary to isolate the intermediates for this synthetic route.

Homodinuclear complexes containing the already mentioned bridging groups were prepared by reacting the corresponding metal acetates with an excess of the cyclic amine in methanol. Addition of bulky anions, viz. ClO_4^-, afforded the homodinuclear complexes. We have already described the homodinuclear Fe(II)–Fe(II) complex containing a μ-hydroxo bridge and two acetate bridges.[7] The Ni(II)–Ni(II) complex will be dealt with in some detail in a forthcoming paper. We are concerned in this paper only with the homodinuclear Cr(III)–Cr(III) complex.

The color of the heterometal dinuclear complexes is red-violet and is dominated by the $Cr^{III}N_3O_3$ chromophore. They are completely air-stable in the solid state, at least for 2 weeks, although the solutions appeared to be slightly air-sensitive. The IR spectra of these compounds are very similar throughout the range 4000–400 cm^{-1}. Besides ligand and ClO_4 absorptions, each spectrum exhibits a sharp, strong band at 3560–3580 cm^{-1} due to ν(OH). One of the characteristics in the infrared spectra of the heterodinuclear Cr(III)–M(II) complexes is a very strong carbonyl stretching vibration found at 1610–1630 cm^{-1}. There is a shift of this ν(CO) to lower frequency at 1560–1570 cm^{-1} for the homodinuclear Cr(III)–Cr(III) complex.

Electronic Spectra. The absorption spectra for the binuclear complexes have been measured both in solution (Figures 1 and 2) and in the solid state. The absorption maxima with the corresponding extinction coefficients in acetonitrile solutions are given in Table VI. The diffuse reflectance spectra measured as KBr disks agree completely with the solution spectra, showing that no dissociation of the binuclear units occurs in the solution. In all of them the bands, attributable to the 6-fold coordinated chromium(III) chromophores,[16] are present, viz. at 18 200–19 300 and 23 800–24 800 cm^{-1}. We may thus correlate the observed electronic spectra directly with the d–d transitions in the ligand field model of configuration d^3, noting that the band assignments have

(14) Computations were carried out on a NOVA (General Data) computer using the SHELXTL program package (revision 3, July, 1981) by G. M. Sheldrick, Universität Göttingen.

(15) *International Tables for X-ray Crystallography*; Kynoch: Birmingham, England, 1974; Vol. 4.

(16) Lever, A. B. P. *Inorganic Electronic Spectroscopy*; Elsevier: Amsterdam, 1984.

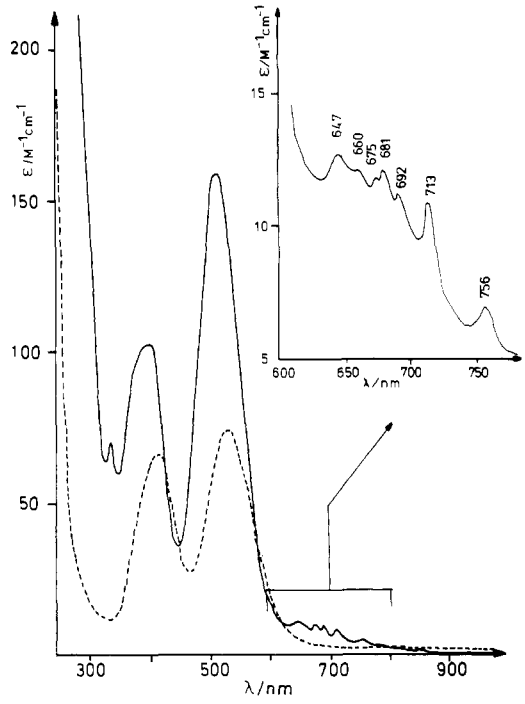

Figure 1. Electronic spectra of $[LCr(OH)(CH_3COO)_2ZnL](ClO_4)_2$ (- - -) and of $[LCr(OH)(CH_3COO)_2CrL](ClO_4)_3$ (—) in acetonitrile solution.

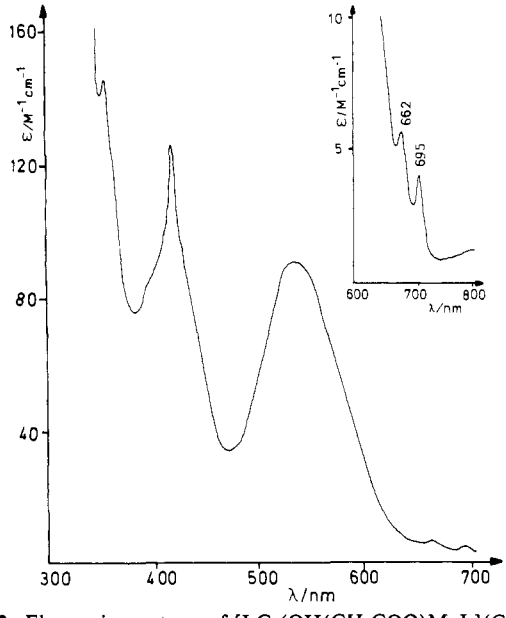

Figure 2. Electronic spectrum of $[LCr(OH(CH_3COO)MnL](ClO_4)_2$ in acetonitrile solution.

been performed by assuming octahedral ligand field states. Let us first consider the dinuclear complex containing the d^3 and d^{10} configured metal ions, viz. $[LCr(OH)(CH_3COO)_2ZnL](ClO_4)_2$. This compound may be considered as the mononuclear counterpart of the corresponding Cr(III)–Cr(III) dimer. The band at 18.7 $\times 10^3$ cm^{-1} (532 nm) is assigned to the first spin-allowed transition $^4A_{2g}(t_{2g}^3) \rightarrow {}^4T_{2g}(t_{2g}^2e_g^1)$ and allows us to approximate the octahedral splitting parameter $\Delta_{oct} \approx 18\,700$ cm^{-1}, which lies between those of the pure $Cr^{III}O_6$ and $Cr^{III}N_6$ chromophores.[17] The second spin-allowed transition $^4A_{2g} \rightarrow {}^4T_{1g}$ occurs at ~24 000 cm^{-1}.

Usually spin-allowed and spin-forbidden d–d bands are observed essentially at the same positions in the dinuclear complex as in the mononuclear complex though the intensity gain of the spin-forbidden transitions through cooperative exchange processes in the dinuclear complex may be considerable.[18] The positions of the two spin-allowed ligand field bands in the homodinuclear Cr(III)–Cr(III) complex remain roughly constant. An interesting feature is the presence of at least seven very weak absorptions (ϵ between 6.8 and 12.5 L mol^{-1} cm^{-1}) in the 13.2 $\times 10^3$ to 15.5 $\times 10^3$ cm^{-1} region, which should be attributed to the spin-flip $^4A_{2g} \rightarrow {}^2E_g$ transitions with intensity gain from exchange coupling. The 800–630-nm absorption of the dinuclear Cr(III)–Cr(III) complex corresponds to the pair of excitations ($^4A_{2g} \rightarrow {}^2E_g$, $^2T_{1g}$) of a $3d^3$ configuration in an octahedral field. The insert of Figure 1 shows an amplified version of the ^2E_g and $^2T_{1g}$ absorption regions in $[LCr(OH)(CH_3COO)_2CrL](ClO_4)_3$. Since transitions to $^2T_{1g}$ are found to be broader than ^2E_g transitions in Cr(III) spectra, it is tempting to assign the lowest energy pair excitation bands at 756 and 713 nm as pure $^4A_{2g}{}^4A_{2g} \rightarrow {}^2E_g{}^4A_{2g}$ transitions. Perturbations by the nearby $^2T_{1g}{}^4A_{2g}$ excitations are assumed to be small.

The spectrum of the heterodinuclear Cr(III)—Ni(II) complex is dominated by the bands of octahedral Cr(III) chromophore. There are small, but not negligible, shifts in the absorption maxima of the heterodinuclear complexes, e.g. Cr(III)–Ni(II), in comparison to those of the corresponding homodinuclear complexes. In addition to the bands due to a nearly octahedral chromium(III) center, an additional band attributable either to copper(II) or to high-spin cobalt(II) is observed in the corresponding heterodinuclear Cr(III)–Cu(II) and Cr(III)–Co(II) complexes, respectively. The absorption spectrum of the Cr(III)–Fe(II) complex consists of many shoulders as is documented in Table VI.

In the heterodinuclear complex containing chromium(III) and manganese(II) centers, two low-energy bands at ~695 and 662 nm with very low intensities are observed and they can be attributed to the spin-forbidden transitions belonging to the chromium(III) center (loc. cit.). Interestingly, a very sharp band with a comparatively high molar absorptivity ($\epsilon \sim 123$ M^{-1} cm^{-1}) occurs at 420 nm (Figure 2). The sharpness of the band clearly shows the spin-forbidden nature of the transition.[16]

This band is thus assignable to the single excitation ($^6A_{1g} \rightarrow {}^4E_g{}^4A_{1g}$) at the Mn(II) center. The components pair of the ^4G term belonging to Mn(II) is degenerate in octahedral symmetry.[16]

Magnetic Studies. The magnetic properties of the exchange-coupled dinuclear complexes have been studied by using the Heisenberg–Dirac–Van Vleck (HDVV) model as simplified to the isotropic Hamiltonian for the case of dimers

$$\hat{H} = -2J\hat{S}_1 \cdot \hat{S}_2$$

Variable temperature (4–300 K) magnetic susceptibility data were fit to the corresponding molar magnetic susceptibility expressions.[19] A correction for a small quantity of paramagnetic impurities had to be taken for a good fit to the data. The expression used is

$$\chi_{calcd}{}^{dimer} = (1 - P_{Cr} - P_M)\left[\frac{C}{T - \Theta} f(J,T)\right] + P_{Cr}\chi_{Cr} + P_M\chi_M$$

where P is the percent of the paramagnetic impurities, $C = Ng^2\mu_B{}^2/k$, and $f(J,T)$ is given in the literature.[19] The observed intradimer exchange integrals are listed in Table VII. Magnetic susceptibility data together with the best fits of theoretical expressions for the exchange coupling between spins $S_1 = {}^3/_2$ and $S_2 = X$ ($X = {}^1/_2$, 1, ${}^3/_2$, and 2) are shown in Figures 3 and 4. The

(17) Jørgensen, C. K. *Oxidation Numbers and Oxidation States*; Springer Verlag: Berlin, 1969.

(18) Decurtins, S.; Güdel, H. U. *Inorg. Chem.* **1982**, *21*, 3598–3606.

(19) O'Connor, C. J.; *Prog. Inorg. Chem.* **1982**, *29*, 203–283.

(20) We have already prepared the Cr(III)–Mn(III) complex, which is presumably an oxo-bridged heterometal dinuclear complex. Interestingly, there seems to be no magnetic exchange interactions between the d^3 Cr(III) and high-spin d^4 Mn(III) metal ions.

(21) Wilkins, R. G.; Harrington, P. C. *Adv. Inorg. Biochem.* **1983**, *5*, 51–85.

(22) Reem, R. C.; Solomon, E. I. *J. Am. Chem. Soc.* **1987**, *109*, 1216–1226 and references therein.

(23) On the basis of the same strategy, the synthesis of the heterodinuclear complex $[L(Cl)Cr(\mu\text{-}OH)_2CuL](ClO_4)_2$ containing a hexacoordinated chromium(III) and a pentacoordinated copper(II) has already been achieved.

Table II. Atomic Coordinates ($\times 10^4$) for $[LCr(OH)(CH_3COO)_2FeL]_2(ClO_4)_4 \cdot H_2O$

atom	x	y	z	atom	x	y	z
Fe(1)	3336 (2)	8173 (1)	3609 (1)	N(7)	2371 (10)	3625 (7)	1136 (6)
Cr(1)	1030 (2)	7445 (2)	3996 (1)	N(8)	2432 (9)	2162 (7)	2078 (6)
O(1)	2524 (7)	7407 (6)	3362 (5)	N(9)	3782 (10)	1907 (8)	601 (6)
O(2)	375 (8)	8738 (6)	4089 (5)	C(21)	2555 (15)	3657 (11)	1844 (8)
O(3)	1559 (8)	7256 (6)	4871 (5)	C(22)	2222 (15)	3040 (10)	2381 (9)
O(4)	1810 (8)	9279 (6)	3626 (6)	C(23)	3703 (14)	1615 (11)	1894 (9)
O(5)	2822 (9)	7961 (7)	4710 (5)	C(24)	4205 (15)	1302 (10)	1177 (9)
C(51)	2262 (13)	7517 (9)	5065 (8)	C(25)	4280 (15)	2597 (10)	480 (10)
C(52)	2412 (16)	7250 (12)	5825 (9)	C(26)	3414 (13)	3502 (10)	555 (8)
C(53)	782 (13)	9356 (9)	3872 (8)	C(27)	1421 (14)	4479 (10)	1032 (9)
C(54)	−133 (15)	10266 (10)	3931 (10)	C(28)	1763 (13)	1707 (10)	2604 (8)
N(1)	4222 (10)	9015 (8)	3864 (7)	C(29)	4094 (15)	1417 (11)	−40 (8)
N(2)	5123 (10)	7186 (8)	3519 (7)	N(10)	−2024 (9)	2384 (7)	1895 (6)
N(3)	4237 (10)	8451 (8)	2496 (7)	N(11)	−2289 (10)	3985 (7)	1162 (6)
C(1)	5244 (17)	8426 (12)	4087 (11)	N(12)	−2069 (9)	2482 (7)	449 (5)
C(2)	5781 (16)	7553 (12)	3854 (10)	C(41)	−2659 (12)	3214 (9)	2332 (8)
C(3)	5682 (17)	7019 (12)	2774 (10)	C(42)	−3173 (12)	3973 (9)	1873 (7)
C(4)	5341 (15)	7707 (11)	2256 (9)	C(43)	−2800 (12)	4089 (9)	533 (7)
C(5)	4435 (17)	9242 (12)	2556 (11)	C(44)	−3101 (11)	3295 (8)	442 (7)
C(6)	4630 (18)	9422 (13)	3177 (10)	C(45)	−2433 (13)	1796 (9)	901 (7)
C(7)	3517 (18)	9661 (12)	4437 (11)	C(46)	−2893 (12)	2068 (9)	1690 (7)
C(8)	5120 (17)	6366 (11)	3887 (10)	C(47)	−1365 (14)	1690 (10)	2338 (8)
C(9)	3533 (16)	8548 (12)	1975 (10)	C(48)	−1882 (13)	4723 (9)	1157 (8)
N(4)	−632 (9)	7453 (7)	4653 (6)	C(49)	−1455 (13)	2134 (10)	−307 (7)
N(5)	1390 (11)	6092 (8)	3941 (7)	Cl(1)	7704 (4)	9400 (3)	1603 (3)
N(6)	238 (10)	7491 (9)	3154 (7)	O(11)	7705 (11)	8704 (8)	2073 (7)
C(11)	−499 (17)	6541 (12)	4832 (11)	O(12)	6781 (16)	10105 (12)	1824 (10)
C(12)	565 (16)	5876 (12)	4550 (10)	O(13)	8716 (16)	9567 (11)	1377 (10)
C(13)	1180 (17)	5924 (12)	3247 (10)	O(14)	7418 (29)	9272 (21)	999 (18)
C(14)	750 (18)	6595 (12)	2846 (11)	Cl(2)	8775 (4)	4809 (3)	3232 (3)
C(15)	−1077 (15)	7737 (12)	3474 (10)	O(21)	9741 (19)	4501 (13)	3545 (11)
C(16)	−1487 (17)	7858 (13)	4226 (11)	O(22)	8005 (26)	5021 (18)	3791 (15)
C(17)	−1066 (15)	7968 (11)	5343 (9)	O(23)	8825 (18)	5514 (13)	2806 (11)
C(18)	2597 (14)	5503 (11)	3979 (10)	O(24)	9029 (19)	4062 (14)	2834 (12)
C(19)	414 (18)	8159 (12)	2604 (10)	Cl(3)	4015 (4)	5915 (4)	1435 (3)
Fe(2)	1832 (2)	2495 (1)	1070 (1)	O(31)	4049 (3)	5905 (9)	2167 (8)
Cr(2)	−926 (2)	2737 (1)	971 (1)	O(32)	4978 (14)	6140 (10)	1027 (9)
O(6)	37 (7)	2976 (5)	1494 (5)	O(33)	2935 (20)	6455 (15)	1414 (12)
O(7)	−202 (7)	3175 (6)	34 (4)	O(34)	4270 (17)	5071 (13)	1200 (11)
O(8)	88 (7)	1505 (5)	761 (5)	Cl(4)	4417 (5)	2487 (4)	3723 (3)
O(9)	1679 (8)	2860 (7)	20 (5)	O(41)	3561 (21)	2963 (15)	4268 (13)
O(10)	1813 (8)	1229 (5)	1012 (5)	O(42)	4520 (17)	2961 (12)	3102 (10)
C(55)	851 (12)	3084 (9)	−276 (7)	O(43)	4039 (18)	1818 (13)	3600 (11)
C(56)	1116 (13)	3280 (9)	−1069 (7)	O(44)	5501 (19)	2058 (13)	3850 (11)
C(57)	1075 (12)	1004 (8)	833 (7)	AQ	7058 (16)	163 (11)	3537 (10)
C(58)	1388 (15)	47 (9)	667 (9)				

magnetic data reflect weak antiferromagnetic exchange coupling interactions, which are expected in view of the superexchange pathways provided by the three bridging ligands.

In the Cr(III)–Zn(II) complex, only the Cr(III) ion is magnetic and has the $^4A_2$ ground state in the trigonal (C_{3v}) environments. The Curie law is obeyed between 110 and 300 K with $\chi_M T = 1.77$ (2) $\times 10^3$ cm^3 mol^{-1} K, the molar effective magnetic moment being constant ($\sim 3.73\ \mu_B$) throughout this temperature range.

In the case of the Cr(III)–Cr(III) complex, we had to use a different Hamiltonian containing a biquadratic term to obtain a good fit of the data to the theoretical susceptibility equation.[24] The Hamiltonian describing the exchange coupling in bimetallic chromium(III) is

$$\hat{\mathbf{H}} = -2J\hat{\mathbf{S}}_1 \cdot \hat{\mathbf{S}}_2 - j(\hat{\mathbf{S}}_1 \cdot \hat{\mathbf{S}}_2)^2$$

where j is the biquadratic coupling constant. The best fit (Figure 3) to the data yielded $J = -15.5$ cm^{-1}, $j = -0.9$ cm^{-1}, and $g = 2.16$. On the basis of the HDVV model, spin–spin coupling between the $S = {}^3/_2$ spin ground states of the two Cr(III) centers would result in four different spin states from $S = 0$ to $S = 3$ in the coupled system. From the magnetic susceptibility data for the Cr(III)–Cr(III) homodinuclear complex, we have derived that the excited spin states are positioned at about $E_1 \approx 25$ cm^{-1} ($S = 1$), $E_2 \approx 81$ cm^{-1} ($S = 2$), and $E_3 \approx 178$ cm^{-1} ($S = 3$).

It should be pointed out that the above approach of the spin-only isotropic model is not strictly applicable for the estimation of J to octahedral cobalt(II) complexes since it ignores the effect of spin–orbit coupling within the $^4T_{1g}$ ground term. The $^4T_{1g}$ ground term of octahedrally coordinated Co(II) splits to form a Kramers doublet ground state under the influence of spin–orbit coupling. Our low-temperature (4–100 K) magnetic data for the Cr(III)–Co(II) complex could not be fitted to the theoretical expression[19] derived from the simple Heisenberg model, showing the complexity of the cryomagnetic behavior. Only the data in the range 100–300 K could be fitted to the susceptibility equation to yield an approximate value of J (ca. −13 cm^{-1}) for the Cr(III)–Co(II) complex. It has previously been noted[25] that the spin-only approach used above may overestimate the value of J by as much as a factor of 2; hence, we have not listed this value in Table VII.

It appears difficult at present to give an interpretation to the relative order of magnitude of J values, obtained from a qualitative analysis. However, this reflects the delicate balance between ferro- and antiferromagnetic interactions in dinuclear complexes. This is of particular importance in systems with a large number of unpaired d electrons as with Mn(II), d^5, because there are an

(24) Hodgson, D. *Prog. Inorg. Chem.* **1975**, *19*, 186.

(25) (a) Kahn, O.; Toal, P.; Coudanne, H. *Chem. Phys.* **1979**, *42*, 355–362. (b) Andrew, J. E.; Ball, P. W.; Blake, A. B. *J. Chem. Soc. D* **1969**, 143–144.

Table III. Atomic Coordinates for $[LCr(OH)(CH_3COO)_2CoL]_2(ClO_4)_4 \cdot H_2O$

atom	x	y	z	atom	x	y	z
Co(1)	0.33556 (12)	0.81766 (9)	0.35919 (7)	N(11)	0.3784 (7)	0.1903 (5)	0.0605 (4)
Cr(1)	0.10344 (13)	0.74312 (10)	0.39885 (8)	N(12)	0.2404 (7)	0.2174 (5)	0.2071 (4)
O(1)	0.1821 (6)	0.9271 (4)	0.3604 (4)	N(13)	0.2311 (7)	0.3636 (5)	0.1132 (4)
O(2)	0.0396 (6)	0.8714 (4)	0.4081 (4)	C(31)	0.4207 (10)	0.1307 (8)	0.1159 (6)
O(3)	0.2788 (7)	0.8010 (5)	0.4688 (4)	C(32)	0.370 (1)	0.1608 (8)	0.1892 (7)
O(4)	0.1598 (6)	0.7241 (5)	0.4860 (3)	C(33)	0.221 (1)	0.3050 (7)	0.2378 (7)
O(5)	0.2551 (5)	0.7387 (4)	0.3354 (3)	C(34)	0.250 (1)	0.3667 (8)	0.1857 (6)
C(1)	0.0778 (9)	0.9346 (7)	0.3874 (6)	C(35)	0.339 (1)	0.3495 (7)	0.0564 (7)
C(2)	−0.0151 (10)	0.0242 (7)	0.3930 (7)	C(36)	0.425 (1)	0.2621 (8)	0.0472 (7)
C(3)	0.2249 (10)	0.7551 (7)	0.5054 (5)	C(37)	0.411 (1)	0.1412 (8)	−0.0034 (6)
C(4)	0.238 (1)	0.7322 (9)	0.5817 (6)	C(38)	0.174 (1)	0.1718 (8)	0.2591 (6)
N(1)	0.5094 (7)	0.7200 (5)	0.3527 (5)	C(39)	0.138 (1)	0.4450 (6)	0.0990 (7)
N(2)	0.4220 (7)	0.8420 (6)	0.2475 (5)	N(14)	−0.2064 (6)	0.2472 (5)	0.0457 (4)
N(3)	0.4207 (7)	0.9016 (5)	0.3840 (5)	N(15)	−0.1998 (7)	0.2366 (5)	0.1898 (4)
C(11)	0.562 (2)	0.6990 (9)	0.2776 (8)	N(16)	−0.2283 (7)	0.3965 (5)	0.1170 (4)
C(12)	0.533 (1)	0.7672 (8)	0.2238 (7)	C(41)	−0.3083 (8)	0.3285 (6)	0.0446 (5)
C(13)	0.439 (1)	0.9244 (8)	0.2545 (8)	C(42)	−0.2809 (9)	0.4088 (6)	0.0548 (5)
C(14)	0.464 (2)	0.9420 (10)	0.3158 (8)	C(43)	−0.3159 (9)	0.3955 (6)	0.1884 (5)
C(15)	0.518 (1)	0.8441 (9)	0.4091 (9)	C(44)	−0.2622 (9)	0.3200 (6)	0.2337 (5)
C(16)	0.575 (1)	0.7562 (9)	0.3829 (8)	C(45)	−0.2879 (9)	0.2062 (6)	0.1693 (6)
C(17)	0.506 (1)	0.6390 (8)	0.3929 (8)	C(46)	−0.2405 (9)	0.1785 (6)	0.0902 (6)
C(18)	0.346 (1)	0.8538 (10)	0.1998 (6)	C(47)	−0.1458 (10)	0.2133 (7)	−0.0296 (5)
C(19)	0.343 (1)	0.9716 (9)	0.4367 (9)	C(48)	−0.1308 (9)	0.1656 (6)	0.2327 (5)
N(4)	0.0242 (8)	0.7498 (6)	0.3165 (5)	C(49)	−0.1854 (9)	0.4712 (6)	0.1167 (6)
N(5)	−0.0625 (7)	0.7442 (5)	0.4646 (4)	Cl(1)	0.7682 (3)	0.9405 (2)	0.1618 (2)
N(6)	0.1390 (7)	0.6096 (6)	0.3949 (5)	O(11)	0.7688 (9)	0.8693 (6)	0.2073 (5)
C(21)	−0.105 (1)	0.776 (1)	0.3493 (6)	O(12)	0.677 (1)	0.0128 (9)	0.1861 (8)
C(22)	−0.148 (1)	0.783 (1)	0.4216 (7)	O(13)	0.873 (1)	0.9528 (8)	0.1373 (7)
C(23)	−0.051 (1)	0.6532 (9)	0.4823 (9)	O(14)	0.727 (2)	0.932 (2)	0.101 (1)
C(24)	0.058 (1)	0.5870 (8)	0.4550 (7)	Cl(2)	0.8757 (3)	0.4813 (2)	0.3250 (2)
C(25)	0.118 (2)	0.594 (1)	0.3240 (9)	O(21)	0.974 (2)	0.4488 (10)	0.3549 (8)
C(26)	0.075 (2)	0.664 (1)	0.2811 (10)	O(22)	0.897 (2)	0.408 (1)	0.2835 (8)
C(27)	0.045 (1)	0.8143 (10)	0.2600 (7)	O(23)	0.879 (2)	0.550 (1)	0.2826 (9)
C(28)	−0.105 (1)	0.7971 (9)	0.5315 (6)	O(24)	0.788 (2)	0.496 (1)	0.379 (1)
C(29)	0.262 (1)	0.5522 (8)	0.3962 (8)	Cl(3)	0.4004 (3)	0.5869 (3)	0.1425 (2)
Co(2)	0.1870 (1)	0.2473 (1)	0.10684 (7)	O(31)	0.404 (1)	0.5904 (7)	0.2145 (6)
Cr(2)	−0.0925 (1)	0.27325 (9)	0.09740 (7)	O(32)	0.487 (1)	0.6122 (8)	0.0971 (6)
O(6)	0.1706 (6)	0.2789 (4)	0.0019 (4)	O(33)	0.430 (1)	0.500 (1)	0.1258 (8)
O(7)	−0.0199 (5)	0.3174 (4)	0.0044 (3)	O(34)	0.292 (2)	0.638 (1)	0.1384 (8)
O(8)	0.0102 (6)	0.1502 (4)	0.0751 (3)	Cl(4)	0.4384 (4)	0.2500 (4)	0.3730 (3)
O(9)	0.1821 (6)	0.1225 (4)	0.1011 (4)	O(41)	0.449 (1)	0.300 (1)	0.3086 (9)
O(10)	0.0071 (5)	0.2946 (4)	0.1496 (3)	O(42)	0.404 (2)	0.181 (1)	0.3560 (9)
C(5)	0.0867 (8)	0.3054 (6)	−0.0280 (5)	O(43)	0.547 (2)	0.212 (1)	0.385 (1)
C(6)	0.1144 (9)	0.3272 (6)	−0.1059 (5)	O(44)	0.355 (2)	0.299 (1)	0.426 (1)
C(7)	0.1098 (10)	0.0994 (6)	0.0819 (5)	O_w	0.707 (1)	0.0169 (8)	0.3588 (7)
C(8)	0.141 (1)	0.0044 (6)	0.0650 (6)				

increasing number of ferromagnetic exchange pathways to consider.

Since the magnitude of the exchange interaction is weak, the zero-field splitting is certainly not without influence on the magnetic properties. The important point, however, is that these data show unambiguously that the metal ions interact in an antiferromagnetic fashion. These systems are good examples of the situation where so many factors are at work that single-crystal susceptibilities are required for a final analysis of the situation.

Electrochemistry. The electrochemical properties of the binuclear complexes were investigated by means of cyclic voltammetry in acetonitrile at 22 °C. The relevant electrochemical data set out in Table VIII clearly indicate that in terms of formal redox potentials [$E^\circ = 0.5\ (E_{p,a} + E_{p,c})$], as well as separation of peak potentials [$\Delta E = E_{p,c} - E_{p,a}$], the electrochemical responses observed with the two electrodes were identical. Because of the absorption problem on the electrode, the Cr(III)–Co(II) complex could not be measured with a Pt electrode. In general, irrespective of the electrodes used, the single one-electron transfer occurs quasi-reversibly as is evident from the adherence to the following criteria: (i) the E° values were independent of scan rates, (ii) the ΔE values increased with scan rates and were always greater than 60 mV, (iii) the ratio of the peak currents due to cathodic ($i_{p,c}$) and anodic ($i_{p,a}$) sweeps were close to unity at different scan rates, and (iv) the product $i_{p,c}\, v^{-1/2}$ remained constant. The formal redox potentials thus obtained can be regarded as thermodynamic values.

The quasi-reversible redox waves are assigned to the Cr(III)–M(II)/Cr(III)–M(III) processes. In this connection, it is to be noted that the E° values indicate the possibility of synthesizing chemically the Cr(III)–M(III) (M = Mn, Fe, Co) dinuclear complexes.[24]

Structure of $[LCr(OH)(CH_3COO)_2FeL](ClO_4)_2 \cdot 0.5H_2O$. The molecular geometry and the atomic labeling scheme of the cation $[LCr(OH)(CH_3COO)_2FeL]^{2+}$ are shown in Figure 6. The X-ray structure confirms that a mixed-metal Cr(III)–Fe(II) complex has indeed been formed in such a way that a confacial bioctahedron geometry containing a chromium(III) and an iron(II) as central atoms is present in the lattice. The two metal ions are bridged by one hydroxo group and two acetate groups. Bond distances and bond angles are listed in Table IV. The structure consists of two distinct mixed-metal cations $[LCr(OH)(CH_3COO)_2FeL]^{2+}$, four noncoordinatively bound statistically disordered perchlorate anions, and a molecule of water of crystallization. Two facially coordinated tridentate amine ligands complete the distorted octahedral coordination sphere of the Cr(III) and the Fe(II) centers. An average Cr···Fe separation of 3.413 (4) Å has been found. The Fe–O (average 2.06 (3) Å) and Fe–N (average 2.21 (0.6) Å) bond lengths correspond to those of the model compound[7] for the diiron centers in deoxyhemerythrin. A deviation from the idealized orthogonal geometry is found for $Me_3[9]aneN_3$, the N–Fe–N angles ranging between 79.6 (5) and 80.1 (4)°, whereas O–Fe–O angles fall between 87.8 (5) and 93.5 (4)°. The bond lengths are consistent with a d^6 high-spin

Table IV. Selected Bond Distances (Å) and Angles (deg) for $[LCr(OH)(CH_3COO)_2FeL](ClO_4)_2 \cdot 0.5H_2O$

Coordination Sphere			
Cr···Fe	3.413 (4)		
Fe(1)–O(1)	2.037 (12)	Fe(1)–N(1)	2.220 (16)
Fe(1)–O(4)	2.090 (8)	Fe(1)–N(2)	2.206 (11)
Fe(1)–O(5)	2.064 (10)	Fe(1)–N(3)	2.212 (12)
Cr(1)–O(1)	1.924 (9)	Cr(1)–N(4)	2.124 (11)
Cr(1)–O(2)	1.959 (9)	Cr(1)–N(5)	2.082 (13)
Cr(1)–O(3)	1.923 (10)	Cr(1)–N(6)	2.102 (15)
O(1)–Fe(1)–O(4)	88.8 (4)	O(4)–Fe(1)–N(1)	90.9 (4)
O(1)–Fe(1)–O(5)	92.9 (4)	O(5)–Fe(1)–N(1)	87.8 (5)
O(4)–Fe(1)–O(5)	93.5 (4)	O(1)–Fe(1)–N(2)	100.6 (5)
O(1)–Fe(1)–N(1)	179.3 (4)	O(4)–Fe(1)–N(2)	169.0 (5)
O(5)–Fe(1)–N(2)	91.7 (4)	N(1)–Fe(1)–N(2)	79.6 (5)
O(1)–Fe(1)–N(3)	99.4 (5)	O(4)–Fe(1)–N(3)	92.8 (4)
O(5)–Fe(1)–N(3)	166.2 (5)	N(1)–Fe(1)–N(3)	79.9 (5)
N(2)–Fe(1)–N(3)	80.1 (4)		
O(1)–Cr(1)–O(2)	94.5 (4)	O(2)–Cr(1)–N(4)	87.1 (4)
O(1)–Cr(1)–O(3)	94.7 (4)	O(3)–Cr(1)–N(4)	87.7 (5)
O(2)–Cr(1)–O(3)	94.8 (5)	O(1)–Cr(1)–N(5)	95.4 (4)
O(1)–Cr(1)–N(4)	177.0 (5)	O(2)–Cr(1)–N(5)	169.0 (5)
O(3)–Cr(1)–N(5)	89.1 (5)	O(3)–Cr(1)–N(6)	167.8 (5)
N(4)–Cr(1)–N(5)	82.8 (5)	N(4)–Cr(1)–N(6)	82.1 (5)
O(1)–Cr(1)–N(6)	95.2 (5)	N(5)–Cr(1)–N(6)	83.0 (6)
O(2)–Cr(1)–N(6)	91.3 (5)		
Bridging Acetate Groups			
C(53)–C(54)	1.494 (18)	C(51)–C(52)	1.521 (23)
C(53)–O(4)	1.215 (18)	C(51)–O(5)	1.226 (20)
C(53)–O(2)	1.278 (20)	C(51)–O(3)	1.264 (23)
O(4)–C(53)–C(54)	118.0 (15)	O(5)–C(51)–C(52)	117.3 (17)
O(4)–C(53)–O(2)	127.3 (12)	O(5)–C(51)–O(3)	127.1 (15)
O(2)–C(53)–C(54)	114.7 (13)	O(3)–C(51)–C(52)	115.6 (15)
Fe(1)–O(4)–C(53)	129.3 (9)	Fe(1)–O(5)–C(51)	132.4 (12)
Cr(1)–O(3)–C(51)	131.8 (9)	Cr(1)–O(2)–C(53)	134.7 (8)
Cr(1)–O(1)–Fe(1)	118.8 (4)		

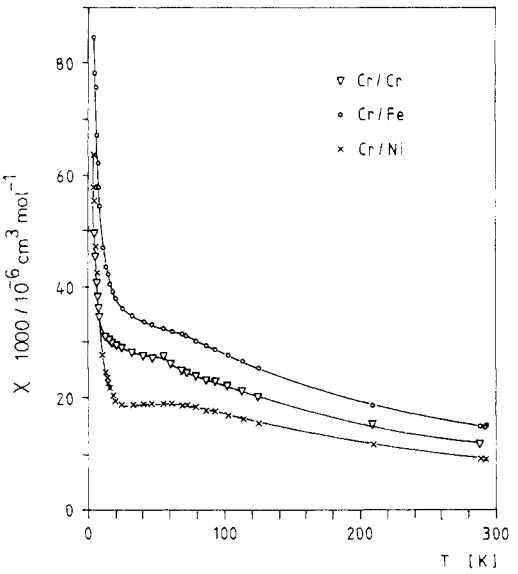

Figure 3. Plot of the magnetic susceptibility vs the temperature for $[L_2Cr_2(OH)(CH_3COO)_2](ClO_4)_3$, $[LCr(OH)(CH_3COO)_2NiL](ClO_4)_2$, and $[LCr(OH)(CH_3COO)_2FeL](ClO_4)_2$: experimental data (×, ○, ▽) and calculated curve (—).

electron configuration of the Fe(II) centers. As expected, the Cr–O and Cr–N bond lengths are significantly shorter.

The octahedral geometry around the chromium center is less distorted than that around the iron (or cobalt, see later) atom. No substantial differences in bond lengths and bond angles are found between the two crystallographically nonequivalent molecules.

Structure of $[LCr(OH)(CH_3COO)_2CoL](ClO_4)_2 \cdot 0.5H_2O$. The structure consists of two discrete heterometal cations [LCr-

Table V. Selected Bond Distances (Å) and Bond Angles (deg) for $[LCr(OH)(CH_3COO)_2CoL](ClO_4)_2 \cdot 0.5H_2O$

Coordination Sphere			
Cr···Co	3.423 (2)		
Co(1)–O(1)	2.086 (7)	Co(1)–N(1)	2.157 (8)
Co(1)–O(3)	2.048 (7)	Co(1)–N(2)	2.188 (8)
Co(1)–O(5)	2.044 (6)	Co(1)–N(3)	2.164 (8)
Cr(1)–O(2)	1.949 (6)	Cr(1)–N(4)	2.052 (8)
Cr(1)–O(4)	1.937 (6)	Cr(1)–N(5)	2.114 (8)
Cr(1)–O(5)	1.937 (6)	Cr(1)–N(6)	2.055 (8)
O(1)–Co(1)–O(3)	91.2 (4)	O(1)–Co(1)–O(5)	89.4 (3)
O(1)–Co(1)–N(3)	90.5 (4)	O(3)–Co(1)–O(5)	92.4 (4)
O(3)–Co(1)–N(3)	87.8 (4)	O(5)–Co(1)–N(1)	99.0 (4)
N(1)–Co(1)–N(2)	81.5 (4)	N(1)–Co(1)–N(3)	81.1 (4)
O(1)–Co(1)–N(1)	170.4 (3)	O(1)–Co(1)–N(2)	93.0 (4)
O(3)–Co(1)–N(1)	92.9 (5)	O(3)–Co(1)–N(2)	169.3 (3)
O(5)–Co(1)–N(2)	97.7 (4)	O(5)–Co(1)–N(3)	180.0 (8)
N(2)–Co(1)–N(3)	82.2 (4)		
O(2)–Cr(1)–O(4)	94.5 (4)	O(2)–Cr(1)–O(5)	94.6 (4)
O(2)–Cr(1)–N(6)	169.4 (3)	O(4)–Cr(1)–O(5)	93.7 (4)
O(4)–Cr(1)–N(6)	88.6 (4)	O(5)–Cr(1)–N(4)	95.4 (4)
N(4)–Cr(1)–N(5)	82.6 (4)	N(4)–Cr(1)–N(6)	84.6 (5)
O(2)–Cr(1)–N(4)	90.8 (4)	O(2)–Cr(1)–N(5)	87.1 (4)
O(4)–Cr(1)–N(4)	169.1 (3)	O(4)–Cr(1)–N(5)	88.2 (4)
O(5)–Cr(1)–N(5)	177.6 (8)	O(5)–Cr(1)–N(6)	95.2 (4)
N(5)–Cr(1)–N(6)	83.0 (4)		
Bridging Acetate Groups			
C(1)–C(2)	1.487 (14)	C(3)–C(4)	1.507 (14)
C(1)–O(1)	1.233 (12)	C(3)–O(3)	1.231 (13)
C(1)–O(2)	1.275 (12)	C(3)–O(4)	1.247 (13)
O(1)–C(1)–O(2)	125.8 (9)	O(3)–C(3)–O(4)	126.9 (9)
O(1)–C(1)–C(2)	118.6 (10)	O(3)–C(3)–C(4)	118.2 (11)
O(2)–C(1)–C(2)	115.3 (11)	O(4)–C(3)–C(4)	115.0 (10)
Co(1)–O(1)–C(1)	129.0 (9)	Co(1)–O(3)–C(3)	133.2 (10)
Cr(1)–O(2)–C(1)	136.5 (11)	Cr(1)–O(4)–C(3)	130.9 (9)
Co(1)–O(5)–Cr(1)	118.6 (1)		

Table VI. Electronic Spectra[a] of Homo- and Heterodinuclear Complexes Containing a Hydroxo Bridge and Two Additional Acetate Bridges in Acetonitrile at 22 °C

	λ_{max}/nm (ϵ/M^{-1} cm^{-1})
$[LCr^{III}(OH)(CH_3COO)_2Zn^{II}L](ClO_4)_2$	532 (73), 416 (67)
$[LCr^{III}(OH)(CH_3COO)_2Cr^{III}L](ClO_4)_3$	756 (6.8), 713 (10.9), 692 (11.1), 681 (12.1), 675 (11.7), 660 (12), 647 (12.6), 517 (160), 404 (103), 375 sh (~100), 338 (70), 312 sh (163)
$[LCr^{III}(OH)(CH_3COO)_2Ni^{II}L](ClO_4)_2$	985 (12), 533 (75), 420 (90), 364 sh (~47)
$[LCr^{III}(OH)(CH_3COO)_2Cu^{II}L](ClO_4)_2$	714 (26), 530 (86), 410 sh
$[LCr^{III}(OH)(CH_3COO)_2Co^{II}L](ClO_4)_2$	1073 (41), 536 (138), 416 (231)
$[LCr^{III}(OH)(CH_3COO)_2Fe^{II}L](ClO_4)_2$	760 sh (18), 730 sh (31), 690 sh (39), 605 sh (89), 550 sh (128), 518 sh (158), 475 sh (194), 420 sh (323), 373 (482)
$[LCr^{III}(OH)(CH_3COO)_2Mn^{II}L](ClO_4)_2$	695 (3.8), 662 (5.3), 536 (89), 420 (123), 356 (143)

[a] Solid-state spectra agree well with these spectra.

Table VII. Magnetic Parameters for Homo- and Heterodinuclear Complexes Bridged by a Hydroxo Ligand and Two Acetate Ligands

compd	J/cm^{-1}	g	P_{Cr}/%	P_M/%
Cr(III)–Cr(III)	−15.5 (5)	2.16 (2)	5.2 (5)	
Cr(III)–Mn(II)	−11.2 (10)	2.00 (4)	1.5 (5)	6.5 (5)
Cr(III)–Fe(II)	−10.6 (5)	2.08 (4)	4.5 (10)	4.5 (10)
Cr(III)–Ni(II)	−18.6 (10)	2.10 (4)	0	0
Cr(III)–Cu(II)	−40 (2)	1.95 (3)	0.5 (2)	0.7 (2)
Cr(III)–Zn(II)	μ_{eff} = 3.71 μ_B (293 K); μ_{eff} = 3.73 μ_B (118 K)			

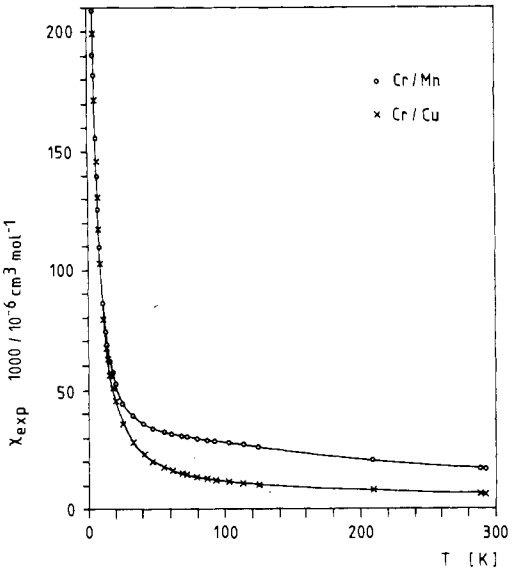

Figure 4. Plot of the magnetic susceptibility vs the temperature for $[LCr(OH)(CH_3COO)_2MnL](ClO_4)_2$ and $[LCr(OH)(CH_3COO)_2CuL](ClO_4)_2$: experimental data (×, O) and calculated curve (—).

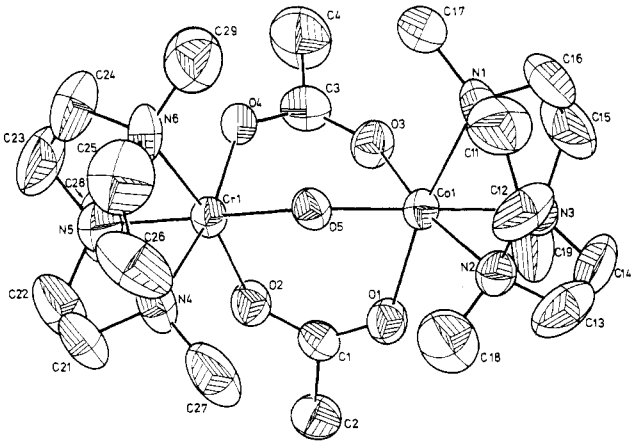

Figure 5. Molecular geometry and atomic labeling scheme of the dication $[LCr(OH)(CH_3COO)_2CoL]^{2+}$ (ellipsoid probability 40%).

Table VIII. Electrochemical Data for the Dinuclear Complexes in MeCN at 22 °C and 0.1 M $(Bu_4N)PF_6$

complex	electrode	scan rates/ mV s^{-1}	ΔE/ mV	$E°$,[a] V vs. Fc^+/Fc^0
Cr(III)-Mn(II)	Pt	20-200	70-80	+0.36
	Au	10-200	65-70	+0.36
Cr(III)-Fe(II)	Pt	10-500	95-125	+0.05
	Au	20-200	80-95	+0.05
Cr(III)-Co(II)	Au	10-500	80-165	+0.03
Cr(III)-Ni(II)	Pt	10-500	irrev oxidn at ca. +1.55 V	
Cr(III)-Cu(II)	Pt	100	irrev oxidn at ca. +1.67 V	
	Pt	100	irrev redn at ca. -0.58 V	
	Au	20-500	irrev redn at ca. -0.55 V	
Cr(III)-Zn(II)	Pt	redox inactive from +2.0 to -1.6 V		
Cr(III)-Cr(III)	Pt	50-200	irrev redn at ca. -0.85 V	

[a] Fc^0 = ferrocene.

$(OH)(CH_3COO)_2CoL]^{2+}$, four uncomplexed statistically disordered perchlorate anions, and a molecule of water of crystallization. The structure of the cation is shown in Figure 5. The cobalt atom is six-coordinated by three nitrogens of the amine ligand and three oxygens of the bridging ligands. An average Cr···Co bond distance of 3.424 (3) Å has been found. The Co–O (average 2.06 (2) Å) and Co–N (average 2.17 (1) Å) bond distances are consistent with a d^7 high-spin electron configuration of the Co(II) center. Selected bond lengths and bond angles are given in Table V. The ligand $Me_3[9]aneN_3$ exhibits no unexpected

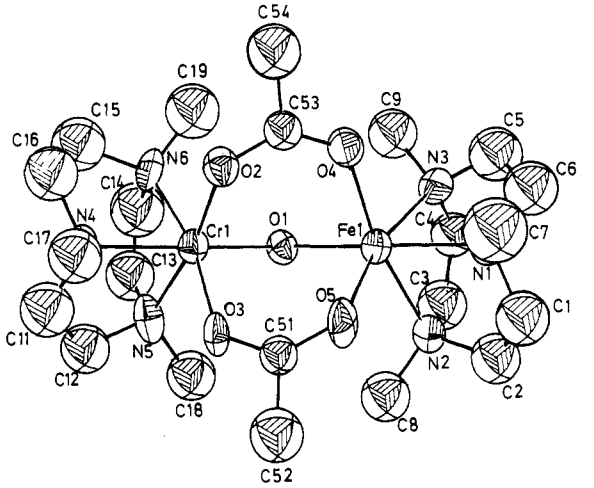

Figure 6. Molecular geometry and atomic labeling scheme of the dication $[LCr(OH)(CH_3COO)_2FeL]^{2+}$ (ellipsoid probability 40%).

Table IX. Unit Cell Parameters for Isotypic Cr(III)–Mn(II) and Cr(III)–Ni(II) Complexes, Space Group $P\bar{1}$ (C_i^1)

	Cr(III)–Mn(II)	Cr(III)–Ni(II)
a, Å	12.674 (3)	12.546 (5)
b, Å	16.290 (4)	16.291 (8)
c, Å	19.224 (6)	19.161 (9)
α, deg	84.47 (2)	84.69 (4)
β, deg	73.91 (2)	74.07 (3)
γ, deg	68.27 (2)	68.55 (3)
V, Å^3	3543 (3)	3505 (3)
Z	4	4
no. of reflcns	25	23
temp, °C	23	23

feature. Comparatively short C–C bond lengths (average 1.39 (6) Å) between the methylene groups of the ligand may be attributed to the effects of libration. The changes observed in the structures between the crystallographically nonequivalent molecules are within experimental error.

Structures of the Cr(III)–Mn(II) and Cr(III)–Ni(II) Complexes. The perchlorate salts of these heterodinuclear complexes are isostructural with the Cr(III)–Co(II) and Cr(III)–Fe(II) complexes. They also crystallize in the triclinic system, space group C_i^1–$P\bar{1}$. The respective unit cell parameters are all very similar and are given in Table IX. It is reasonable to assume that for these complexes also the distorted-octahedral geometry of N_3O_3 donor set around each metal center prevails.

Relatively large distortion can be expected for the Cr(III)–Cu(II) complex, in which the coordination around copper is presumably tetragonally elongated as observed in several mononuclear and dinuclear copper complexes due to the Jahn–Teller effect.

Summary. The following points are the principal results and conclusions of this investigation.

1. We have found a general route to high-yield synthesis for the dinuclear complexes containing the $[M_1M_2(OH)(CH_3COO)_2]$ moiety, where M_1 and M_2 may be similar or dissimilar metal atoms. The inherent stability of this core is indicated by its ready formation in solution. The stability of this moiety, unambiguously identified to be present in the metalloprotein hemerythrin,[21,22] may have a direct bearing on our understanding of the biological molecular evolution. This preparation method can also be used for synthesizing heterodinuclear complexes containing other bridging ligands.[23]

2. The study of the magnetic properties of these complexes indicates that the metal centers are weakly antiferromagnetically coupled.

3. The electronic spectra of the heterodinuclear complexes are not superimpositions of those of their homodinuclear counterparts, presumably because of the metal–metal interactions occurring through the bridging ligands. The intensity gain through exchange coupling seems to be responsible for observation of several spin-

forbidden transitions ($^4A_{2g} \rightarrow {}^2E_g$) of d^3 configuration in an effective octahedral field. A special feature of the Cr(III)–Mn(II) spectrum is a very sharp band at 420 nm ($\epsilon \sim 123$ M^{-1} cm^{-1}), which is assigned to the single excitation ($^6A_1 \rightarrow {}^4E^4A_1$) at the Mn(II) center.

4. The oxidized species Cr(III)–M(III) (M = Mn, Fe, and Co) obtained by the electrochemical oxidation seems to be stable on the voltammetric time scale, and hence, the chemical preparation of the oxidation products should be feasible.

Acknowledgment. We thank the Fonds der Chemischen Industrie for financial support of this work. Our thanks are also due to Prof. Dr. W. Haase and Dipl. Chem. S. Gehring (Darmstadt) for the low-temperature susceptibility measurements.

Supplementary Material Available: Listings of intraligand bond angles and distances, hydrogen atom coordinates, and anisotropic and isotropic thermal parameters for the Cr(III)–Fe(II) complex and anisotropic thermal parameters and hydrogen atom coordinates and isotropic thermal parameters for the Cr(III)–Co(II) complex (20 pages); listings of observed and calculated structure factors (76 pages). Ordering information is given on any current masthead page.

Contribution from the Department of Chemistry and Laboratory for Molecular Structure and Bonding, Texas A&M University, College Station, Texas 77843

Synthesis, Solid-State and Solution Structure, and Physicochemical Properties of the Iodide-Bridged Face-Sharing Bioctahedral Molybdenum(III) Dimers $[Cat]^+[Mo_2I_7(PMe_3)_2]^-$ (Cat = $PHMe_3$, NMe_4, $AsPh_4$)

F. Albert Cotton* and Rinaldo Poli

Received March 13, 1987

The compound $[PHMe_3][Mo_2I_7(PMe_3)_2]$ (**1**) has been obtained from $Mo_2I_4(PMe_3)_4$ and I_2 in toluene. The reaction of $MoI_3(THF)_3$ with PMe_3 and NMe_4I in a 2:2:1 molar ratio affords $[NMe_4][Mo_2I_7(PMe_3)_2]\cdot 2THF$ (**2**) while $[AsPh_4][Mo_2I_7(PMe_3)_2]$ (**3**) has been obtained from **2** by metathesis with $AsPh_4Cl$. Crystal data: for compound **1**, monoclinic, space group $P2_1/n$, a = 12.928 (10) Å, b = 23.206 (12) Å, c = 10.648 (9) Å, β = 110.95 (6)°, V = 2983 (8) Å^3, Z = 4, R = 0.0623 (R_w = 0.0923) for 180 parameters and 2202 unique data having $F_o^2 > 4\sigma(F_o^2)$; for compound **3**, orthorhombic, space group $P2_12_12$, a = 14.347 (3) Å, b = 19.349 (4) Å, c = 8.076 (1) Å, V = 2242.0 (7) Å^3, Z = 2, R = 0.0385 (R_w = 0.0579) for 161 parameters and 1643 unique data having $F_o^2 > 3\sigma(F_o^2)$. The compounds have a face-sharing bioctahedral structure with three bridging iodine atoms and two additional terminal iodine atoms and one phosphine group per molybdenum atom. The phosphine ligands are in the syn configuration in the solid state. Dissolution causes an equilibration with the gauche isomer to the statistical 1:2 mixture, with k_1 = (7.67 ± 0.14) × 10^{-4} s^{-1} and k_{-1} = (3.83 ± 0.07) × 10^{-4} s^{-1} in acetone at 20 °C. The Mo–Mo distance of 3.022 Å for both compounds **1** and **3** indicates a significant metal–metal interaction. The compounds show a temperature-dependent paramagnetism. A variable-temperature ^1H NMR study is reported.

Introduction

We have recently studied the decarbonylation reaction of $MoI_2(CO)_3(PR_3)_2$ materials.[1-4] This reaction led to the formation of dimers containing a quadruple metal–metal bond, $Mo_2I_4(PR_3)_4$ and/or to disproportionation with formation of molybdenum(0) carbonyl derivatives and mononuclear molybdenum(III) iodide–phosphine complexes. Since molybdenum(III) complexes containing iodide had not been thoroughly studied before and are in principle expected to exhibit interesting metal–metal interactions in polynuclear species,[5] we have examined the possibility of obtaining these materials by more selective routes. In pursuit of this goal, we have been able to synthesize the potentially useful tetrahydrofuran adduct $MoI_3(THF)_3$,[6] with the intention of using it as a starting material for ligand substitution reactions. As an alternative strategy, we tried to add I_2 oxidatively to the quadruply bonded molybdenum(II) dimers $Mo_2I_4(PR_3)_4$. The formation of the edge-sharing bioctahedral $Mo_2I_6(dppm)_2$ [dppm = bis(diphenylphosphino)methane] has been recently achieved in this way.[7] Our attempt to prepare a similar edge-sharing bioctahedral $Mo_2I_6(PMe_3)_4$ resulted instead in the formation of the face-sharing bioctahedral $[Mo_2I_7(PMe_3)_2]^-$ ion, as well as other, as yet, uncharacterized products. This chemistry and an alternative synthesis of the anion from $MoI_3(THF)_3$ are reported here, together with structural studies in the solid state (by X-ray techniques) and in solution (by ^1H NMR).

Experimental Section

All operations were performed under an atmosphere of prepurified argon with standard Schlenk-tube techniques. Solvents were purified by conventional methods and distilled under dinitrogen prior to use. Instruments used were as follows: IR, Perkin-Elmer 783; UV/visible, Cary-17; NMR, Varian XL-200. Elemental analyses were by Galbraith Laboratories Inc., Knoxville, TN. Magnetic susceptibility measurements were performed by the Gouy method as modified by D. F. Evans on a JME magnetic balance (Johnson Matthey). The compounds $Mo_2I_4(PMe_3)_4$[1] and $MoI_3(THF)_3$[6] were prepared according to published procedures.

Reaction between $Mo_2I_4(PMe_3)_4$ and I_2 in Toluene. Preparation of $[PHMe_3][Mo_2I_7(PMe_3)_2]$ (1). A 95-mg sample of the molybdenum(II) dimer (0.095 mmol) was treated in toluene (10 mL) with I_2 (24 mg, 0.095 mmol). Stirring at room temperature for a few hours caused no change. The solution was then warmed to the reflux temperature. A brown precipitate formed. This was filtered off and extracted with CH_2Cl_2 (3 mL), and the filtered solution was carefully layered with 5 mL of toluene. The red X-ray quality crystals that formed (compound **1**, 15 mg), were decanted, washed with hexane, and dried in vacuo. Anal. Calcd for $C_9H_{28}I_7Mo_2P_3$: C, 8.25; H, 2.15. Found: C, 8.41; H, 2.23. IR (Nujol mull): 1410 m, 1300 m, 1280 m, 1265 m, 960 s, 790 m, 735 m cm^{-1}.

Reaction of $MoI_3(THF)_3$ with PMe_3 and NMe_4I in a 2:2:1 Molar Ratio. Preparation of $[NMe_4][Mo_2I_7(PMe_3)_2]\cdot 2THF$ (2). $MoI_3(THF)_3$ (1.735 g, 2.50 mmol) was suspended in 20 mL of THF and treated with 0.25 mL of PMe_3 (2.5 mmol) and 0.287 g of NMe_4I (1.23 mmol). The mixture was stirred at room temperature for about 2 h and then refluxed overnight. The color of the solution had changed from red to yellow-

(1) Cotton, F. A.; Poli, R. *J. Am. Chem. Soc.* **1986**, *108*, 5628.
(2) Cotton, F. A.; Poli, R. *Inorg. Chem.* **1986**, *25*, 3624.
(3) Cotton, F. A.; Dunbar, K. R.; Poli, R. *Inorg. Chem.* **1986**, *25*, 3700.
(4) Cotton, F. A.; Poli, R. *Inorg. Chem.* **1986**, *25*, 3703.
(5) (a) Cotton, F. A.; Wilkinson, G. *Advanced Inorganic Chemistry*, 4th ed.; Wiley: New York, 1980; p 864. (b) Cotton, F. A.; Ucko, D. A. *Inorg. Chim. Acta* **1972**, *6*, 161.
(6) Cotton, F. A.; Poli, R. *Inorg. Chem.* **1987**, *26*, 1514.
(7) Cotton, F. A.; Dunbar, K. R., manuscript in preparation.

0020-1669/87/1326-3310$01.50/0